Ibn Al-Haitham Journal for Pure and Applied Sciences
Journal homepage: jih.uobaghdad.edu.iq
PISSN: 1609-4042, EISSN: 2521-3407
IHJPAS. 2026; 39(1)

Optical Characterization of Neem Leaf by Laser Beam Scanning Spectroscopy (LIBS) and its spectral Properties

Noor ALhuda Rafid Hazim[1] and Alyaa Hussein Ali[2*]
[1,2] Department of Physics, College of Science for Women, University of Baghdad, Baghdad, Iraq
*Corresponding Author

Received: 27/May /2025.
Accepted:10/September/2025
Published: 20 /January/2026
doi.org/10.30526/39.1.4216

Abstract

The present investigation is concerned with the spectral characterization by laser-induced bioluminescence spectroscopy (LIBS) of neem (*Azadirachta indica*) generated plasma, which is one of the most versatile and fast methods for the qualitative and quantitative analysis of various chemical elements, in organic as well as organic materials. Sample excitation and plasma formation were achieved using a pulsed energy laser (50, 100, 150, and 200 mJ). Finally, the emitted spectrum was analyzed in the framework of the Boltzmann and Saha equations for obtaining the plasma temperature and electron density. The influence of the laser power on the spectral parameters, for example, spectral line intensity, electron temperature, and electron density, was investigated, which could contribute to knowing more about the interaction between plasma and the component of the plant sample. The results show that LIBS is a fast and reliable tool for the analysis of chemical elements of the Neem sample, and at the same time, it does not require complex sample preparation, so it is suitable for clinical, pharmacological, and environmental applications. The work demonstrates a direct dependency of the laser power, the associated rise in plasma temperature, and corresponding electron density on the sensitivity of the spectrometer, emphasizing the need to optimize these parameters to achieve accurate and highly repeatable measurements.

Keywords: Laser ablation spectroscopy, Laser plasma, Neem (*Azadirachta indica*), Plasma temperature, Electron density.

1. Introduction

Neem, tried to think of its botanical name, yes, *Azadirachta indica*, there are not so many medicinal trees found in India. It is a member of the *Meliaceae* family and can be found in tropical and subtropical regions, and can tolerate arid environments. This tree is reported to possess some vital compounds having insecticidal properties and preventing insects against stored seeds. Meanwhile, some health benefits have long been associated with it, including lowering blood sugar, antiparasitic, anti-inflammatory, ulcer prevention, and liver protection, although there are some side effects in some references. In this decade, there has been a trend of increasing prevalence in the use of herbal drugs as a more preferable medicinal product than chemical and synthetic drugs, with less of their side effects compared to standard antibiotics. Herbs can be applied by direct active components or via plant extracts [1,2]. Neem (*Azadirachta indica*) is a tropical evergreen that has several uses, and thus is a potential source of environmentally friendly pest control, environmentally safe pharmaceuticals, wood, and non-wood products. It has also been found to be successful for afforestation. Neem-based products have gained more popularity in recent years for the control of pests, since their primary biologically active ingredient, azadirachtin, has been shown to have multiple effects, including anti-feeding and ovicidal activity[3,4], causing disruption in the life stages of many insects. Optical

emission spectroscopy (OES) is light gathered, spectrally analysed, and detected. The pulse emitted by plasma can be strong enough that the light collection and detection efficiency does not necessarily require further optimization[4,5]. This analytical method is a well-established and commonly utilized tool for the determination of the elemental composition of most mineral samples[5]. OES is based upon the analysis of the light emitted by a sample to identify its wavelengths, because each individual element has characteristic lines in its spectrum that do not overlap with any other element. Analysis of these lines can determine elemental components in the material and accurately quantify their concentration. This method is widely applied in many fields (physics, chemistry, medicine) to deduce and analyze the material' s composition[6,7]. Optical emission spectroscopy is an accurate method that is capable of offering insight into the properties of materials at an atomic and molecular level and, thus, has found extensive scientific and technical uses. Of the analytical techniques linked to this technique, laser-induced breakdown spectroscopy (LIBS) has proven to be a practical technique for elemental analysis[8,9]. This technique is applicable to all solid, liquid, and gaseous phase media and relies on optical observation of the emission signals emitted by the plasma produced upon the irradiation of the sample with the laser pulse. Atoms, ions, and free electrons, the most important constituents of the plasma, offer a basis for a complete understanding of the elements that constitute the primary building blocks of matter [10,11].

1.1. Theory

A spectrometer and detector are used to observe the light emitted from the plasma produced when the sample material is ionized and eroded by a high-intensity laser pulse. The properties of the emission lines, such as their width, shape, and shifts, can be analyzed to extract important information, including the plasma temperature and electron density[12,13]. The research was carried out using the Boltzmann diagram approach, where the temperature of the generated plasma is an important factor in characterizing its properties. This method is widely used in laser-induced breakdown spectroscopy (LIBS) studies to measure plasma temperatures, especially in thermal systems[14,15] .The principle of this technique is based on the Boltzmann distribution, which describes how particles (such as atoms or ions) are distributed across different energy levels in an equilibrium thermal system. The steps in applying the Boltzmann method include [16]. Collecting spectral data and measuring the intensity of the spectral lines resulting from different energy transitions in the atoms or ions within the sample.

Determining the energy levels of each spectral line, using spectral tables or specialized databases. Application of the Boltzmann equation, which relates the intensity of the spectral line (I), the number of atoms in a given energy level, and the temperature, allows the plasma temperature to be accurately estimated[17,18].

The average temperature of the plasma can be expressed by the temperature (T) as determined using this technique, based on **Equation 1** [19, 20]:

$$T=\frac{(E_2-E_1)}{k\ln(\frac{I_1\lambda_1A_2g_2}{I_2\lambda_2A_1g_1})} \quad \textbf{(1)}$$

The Saha-Boltzmann equation is a fundamental tool for analyzing advanced stages of spectral line ionization. It depends on several factors, including the intensity of the spectral lines (I), the statistical weight (g), the conversion probability (A), as well as the wavelength (λ) and the energy of the excited state (E). The Boltzmann constant (K) also plays an important role in calculating this relationship [20,21]:

$$n_e = \frac{I_1}{I_2^*}\, 6.04\times10^{21}\,(10)^{\frac{3}{2}}\; e^{\frac{(E_1-E_2-X_Z)}{KT}} \quad cm^{-3} \quad \textbf{(2)}$$

$$I_2^* = \frac{I_2\lambda_2}{g_2\,A_2} \quad \textbf{(3)}$$

Where: X_z represents the ionization potential of an organism at the second ionization level, measured in electron volts (eV) [22]. I_2 represents the intensity of the spectral transition from level 2 to level 1, λ is the wavelength associated with this transition, and is considered within the

acceptable range. g_2 Determines the statistical weight of this transition, while A_2 refers to its probability of occurrence. The symbol z is used to indicate the ionization stage of the species studied [23-26]. The frequency of the generated plasma can be calculated using the equation provided for this purpose, [27]:

$$f_p = 8.98\sqrt{n_e} \quad HZ \qquad \textbf{(4)}$$

Plasma frequency is one of its fundamental properties, directly dependent on its density. Typically, low values of n_e Result in a significantly higher plasma frequency[20]. Where charged particles interact to reduce the influence of surrounding electric fields. The Debye length (λ_D) is defined as the distance at which this effect occurs.

Quasi-neutrality in plasmas occurs as a result of the Debye shielding effect, where charged particles reduce the influence of surrounding electric fields. The Debye length (λD) is determined based on this distance [28,29]:

$$\lambda_D = \sqrt{\frac{\epsilon_\circ K_B T_e}{e^2 n_e}} = 7.43\times 10^2 \sqrt{\frac{T_e}{n_e}} \qquad \textbf{(5)}$$

N_D denotes the density of particles at the Debye surface, which depends on the electron density and temperature. The existence of a plasma is conditional upon $N_D >>> 1$[30]:

$$N_d = \frac{4\pi}{3} n_e \lambda_D^3 \qquad \textbf{(6)}$$

2. Materials and Methods

Neem leaves were washed with water and rinsed with distilled water to remove dust and soluble impurities, then left to dry in the open air under shade, at room temperature, until they became crunchy. The dried leaves were then crushed using a mechanical grinder and pressed using a press at 6 Pa for 10 minutes to form granules of 20 mm diameter and similar thickness. The resulting material was used for a plasma spectroscopy study, and its chemical composition was determined using X-ray fluorescence (XRF) analysis, which is based on the analysis of the material to reveal its chemical components. **Figure 1** shows a sample of Neem Leaves.

Figure1. Sample of Neem leaves[4].

2.1. X-ray fluorescence (XRF) analysis

XRF analysis: X-ray fluorescence takes place when primary X-rays stir material, forcing it to emit secondary X-rays. The emitted rays have a characteristic spectrum depending on the elements that compose the material; the latter can then be chemically analyzed (**Table 1).**

Table 1. *Azadirachta indica* (Neem).

Element	Concentration
CaO	7.5680%
K2O	1.7850%
SiO2	1.5130%
SO3	0.6915%
MgO	0.6572%
P2O5	0.5434%
Cl	0.1923%
Al2O3	0.1308%

3. Results

3.1. Neem Optical Emission Spectroscopy (OES) Analysis

Neem uses of OES analysis. Such is the case for laser beam ionization spectroscopy (LIBS) in which a short, high-powered laser pulse impinges on a sample, causing the material to be evaporated, and a plasma of ionized atoms and charged particles is produced. As the plasma cools, the atoms lose their excited states and decay to their lowest energy levels, emitting photons with wavelengths corresponding to each element (shown in a spectrum). The spectral behaviour can be interpreted as follows: to analyze the neem components at various laser energies (50, 100, 150, and 200 mJ) as seen in **Figure 2**. The influence of the laser energy on the intensity of the spectral radiation may be rationalised in terms of increased intensity of the spectral radiation with increasing laser energy, as is illustrated in the enhancement of the spectral peaks in the 200 mJ condition compared to the 50 mJ case. This is because the higher the laser energy, the more material is vaporized and decomposed, so that more ionized atoms are generated in the plasma, with the radiation intensity of the plasma being increased. The visible lines shown by the spectral lines are attributed to the presence of the different elements in the neem tree, like calcium (Ca), potassium (K), silicon (Si), magnesium (Mg), and chlorine (Cl). These constituents may be the components of the chemical composition of the plant, as calcium and potassium are important elements in plants. Spectral lines become sharper and less overlapping as laser power increases. It indicates that increasing energy betters the ionization of various elements and smoothen the plasma. Some spectral lines become sharper at a specific level of energy, while they weaken or disappear at other levels may reflect differences in the degree of ionization of elements. Some elements may require high energy before they can radiate and emit their spectral radiation. Therefore, increasing laser powers increases the intensity of the spectral radiation and deblurs the spectral lines. Spectral lines observed are due to the presence of elements such as Ca, K, and Si produce spectral lines observed on neem due to Mg and Cl.

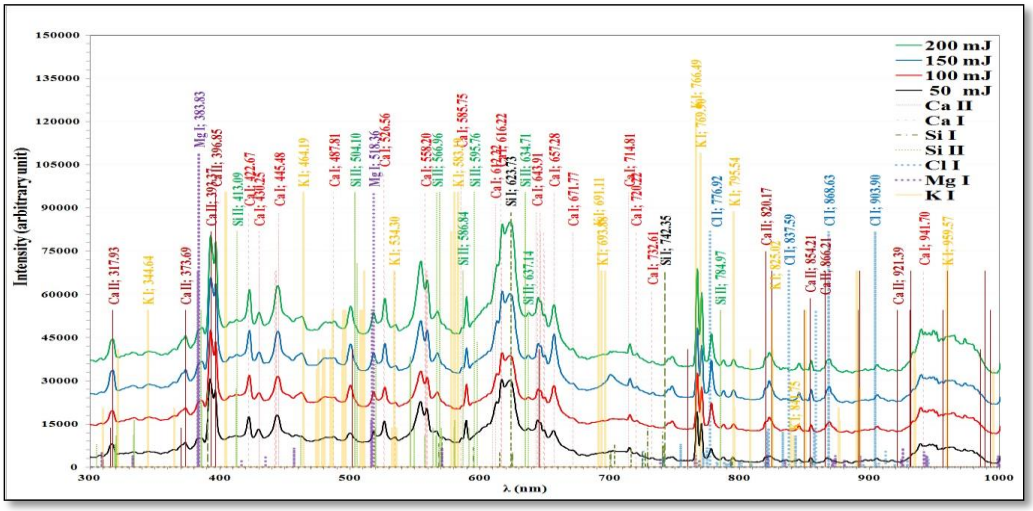

Figure 2. The Neem optical emission spectra.

Figure 3 represents a spectral analysis of the neem herb using laser beam scanning spectroscopy (LIBS) at different laser energies (50, 100, 150, and 200 mJ).

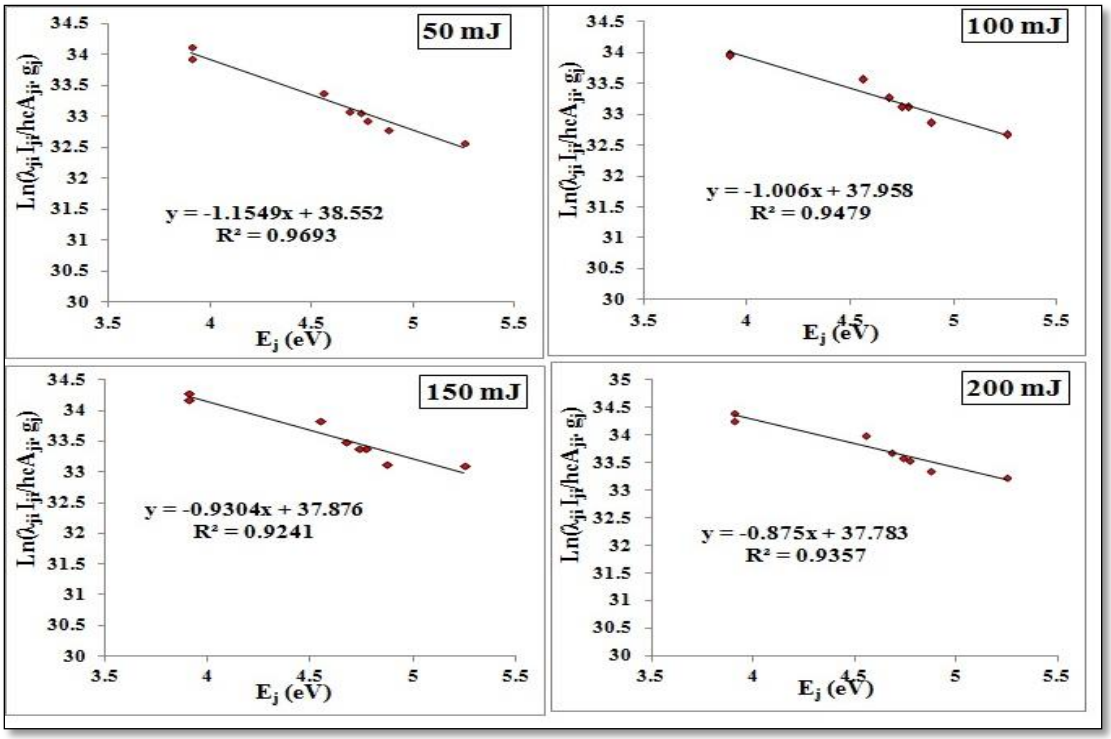

Figure 3. Effect of laser energy on the spectral properties of neem herb using laser beam scanning spectroscopy (LIBS)

The R^2 values was shown in **Table 2** at (50,100,150,200 mJ energy).

Table 2. Determination Coefficient (R^2) of Laser Energy Effect on the Plasma of Neem Herbs Extract.

Energy (mJ)	R^2
50	0.9693
100	0.9479
150	0.9241
200	0.9357

Figure 4 LIPS spectrum of neem at different energies (50mJ, 100mJ, 150mJ, and 200mJ) of laser (LIPS emission of neem sample). The horizontal axis (λ) indicates the wavelength of the emitted light (in nm), that is, the wavelength of the light that the plasma induced by the laser applied to the sample emits. The vertical axis represents the magnitude of a signal in arbitrary units (intensity [arbitrary unit]) proportional to the strength of radiation released from the plasma. The colored curves correspond to the emission spectra of neem at various energies. It is noticed that the signal intensity scales with the pump power. At every different energy, there is a unique emission peak at a specific wavelength. The dashed curves show a fit to a Lorentzian of the functions; as a result of these, the emission lines have a particular profile corresponding to the energy distribution in the plasma. In the spectral line amplitude domain, the spectral peaks appear broader in width with increasing laser power, which is attributed to the Doppler broadening effect or particle collision in the plasma.

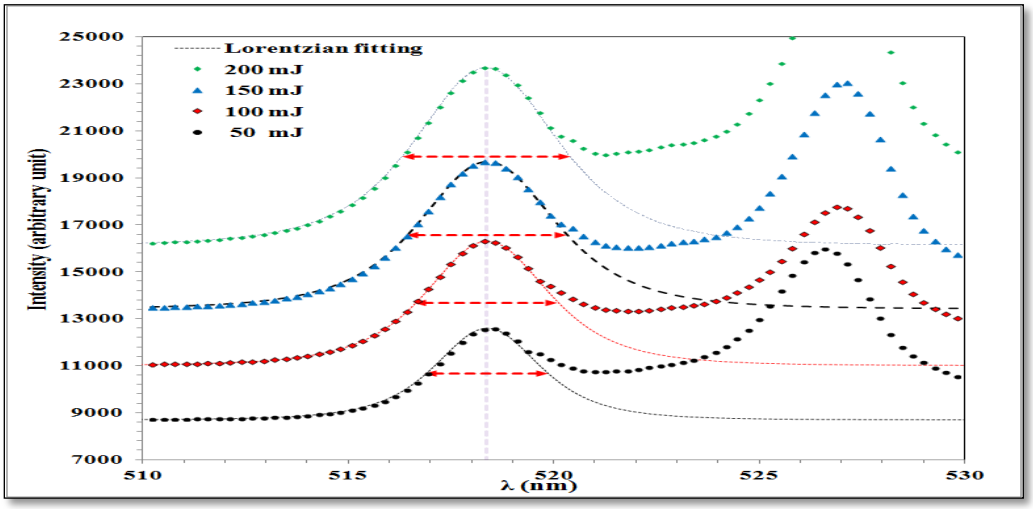

Figure 4. Laser-Induced Plasma Emission (LIPS) Spectrum Analysis of Neem at Different Laser Energies

The action of laser energy on the properties of the plasma produced by analysis of neem can be seen in **Table 3.**

Table 3. Effect of laser energy on plasma parameters of neem extract using the LIBS technique.

Laser energy (mJ)	T_e (eV)	Δλ (nm)	$n_e \times 10^{17}$ (cm^{-3})	f_p (Hz) $\times 10^{12}$	$\lambda_D \times 10^{-6}$(cm)	N_D
50	0.866	3.000	42.857	18.590	3.340	669
100	0.994	3.500	50.000	20.080	3.313	761
150	1.075	3.900	55.714	21.196	3.263	811
200	1.143	4.100	58.571	21.733	3.282	867

While **Figure 5** shows the effect of laser energy on the number density and temperature of electrons in neem extract plasma using LIBS.

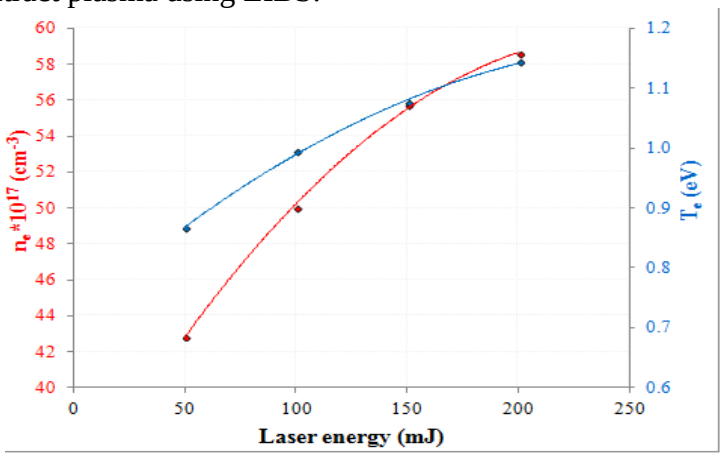

Figure 5. The effect of laser energy on the number density and temperature of electrons in neem extract plasma using LIBS.

4. Discussion

The obtained results are highly effective for studying the chemical identification of the components with high precision. The Effect of Laser Energy on Spectral Line Intensity As the **Figure 2** shown that the laser energy increased from 50mJ to 200mJ, and the spectral line did not become less overlapping. One can describe the spectra as follows:

Descriptions of a few of the features in the spectrum A. Calcium (Ca) Calcium can be observed with several spectral profiles, including: Ca II (317.03, 393.37, 396.85, 854.21, 866.21, 921.39, 941.70 nm) Ca I (422.67, 445.48, 487.81, 534.30, 657.28 nm). As calcium is a critical component of plant cell walls, the existence of this element in the spectrum indicates that neem

is a rich source of this element. As the laser energy increases, the clarity of the image becomes better, suggesting that the ionization of calcium is more effective in high-energy plasma. B. Potassium (K) Potassium lines are visible at many longitudes, for example: KI (373.60, 766.49, 769.54, 766.92, 770.54, 794.57 nm). Potassium is vital for photosynthesis and water uptake in plants, and since potassium is found in the spectrum, that means neem is rich in it! The signal of the potassium lines increases at higher energies, an effect of the greater plasma quantity. C. Silicon (Si): Silicon is present at wavelengths as: Si I (390.55, 508.30, 742.35 nm). Si II (595.76, 637.14, 671.77 nm). Based on comparing spectra showing and not showing hydrogen, and studying the correlation of various absorption lines with luminosity, we propose that there may be significant contributions from LBVs to the recombination spectrum. Silicon is involved in resistance against plant disease and increases the rigidity of the plant. Some Si lines are visible at higher energies, where their abundances should require more ionization. D. Magnesium (Mg): Magnesium is found at: Mg I (383.83, 518.36 nm). Magnesium is also the key element of chlorophyll, essential for plant photosynthesis. Its existence in the spectrum indicates that the neem has a good content of magnesium. E. Chlorine (Cl): Chlorine is found at: Cl I (820.17, 837.59, 868.63, 903.90 nm). Its presence means that the herb contains chlorine compounds, which could be significant in biochemical processes in the plant[11].

Effect of Wavelength Detectable Sensitivity. At wavelengths ward than 400 nm, detection is more sensitive, because lines of more ionized elements, including alternating with $Ca^{(2+)}$ and $Mg^{(2+)}$ soil to appear. Between 600 and 900 nm, lines of more massive elements such as Ca^{2+} and K^{2+} are observed, meaning that these are less ionized lines.

Figure 3 displays the relationship between Ln (αij ħν /Aji - Ej) versus Ej (eV), where αij represents the absorption coefficient, ħν represents the photon energy, Aji represents the transition probability coefficient, and Ej represents the energy levels. The decreasing slope indicates that increasing laser energy results in relatively fewer ionization effects, which may be due to absorption saturation or molecular stability. At higher energies (150 and 200 mJ), some atoms may have reached a maximum ionization state, resulting in reduced additional spectral changes. These changes may be related to the elemental content of the herb, as some organic compounds interact with the laser in a nonlinear manner. The spectral changes indicate the possibility of breaking certain molecular bonds or redistributing electronic energy levels as a result of partial ionization[24].

Explanation of the Declining Slope with Increasing Laser Energy. At 50 mJ, the slope (-1.1549) is higher, indicating that the plasma is still in the strong interaction phase, where absorbed energy increases and electrons are in a highly excited state. At 100 mJ and 150 mJ, the slope decreases to (- -1.006 and -0.9304), indicating a gradual stabilization of the plasma and a change in the rate of electron transition between energy levels. At 200 mJ, the slope is lower (-0.875), indicating that the plasma has become more stable and may have reached the ionization saturation phase, where additional spectral effects are reduced. The chemical Interpretation is that neem contains trace organic and mineral elements. When exposed to a laser with increasing energy. At low energies (50 mJ), there may be slight stimulation of electron transitions, while at higher energies, molecular bonds may begin to break, resulting in a difference in spectral emission. Increased Metal Ionization: the minerals in the sample, such as calcium, potassium, and magnesium, may reach higher ionization levels at higher laser energies, leading to a marked change in absorption properties[21].

At 200 mJ, the plasma becomes more extensive and may reach a steady state where the additional laser effect on the plasma composition is reduced. To improve LIBS technology for analyzing plant compounds, this data can be used to understand the effect of lasers on medicinal plants, helping to develop accurate methods for analyzing the chemical elements within them. The response of neem to lasers depends on the energy used, with low energy resulting in limited electron excitation, while high energy results in saturation ionization and plasma stability. This

study can be used to understand the effect of lasers on bioactive compounds and improve the spectral analysis of neem for use in medical and environmental applications.

The R^2 values in **Table 2**, and the value of 50 mJ is 0.9693. It shows the best accordance between the data and the straight line, and thus the best fit of the plasma diagnosis at this energy. This can be attributed to the low laser power that generates a quite homogeneous plasma, resulting in less spectral dispersion. At 100 mJ, the R2 value is 0.9479. This suggests that a linear model is reasonable, but the fit is slightly less accurate than 50 mJ. This could be a result of interactions in the plasma becoming more dominant as the laser power increases, meaning the measurements are slightly influenced by the more dispersion. At 150 mJ, R^2 is 0.9241 lowest of any energy, again indicating that a linear model is less accurate for modeling the spectral relationship at this energy. This could be caused by higher plasma density, which could induce effects like self-absorption or interaction effects of particles. Overlap of spectral lines because of high ionization. R^2-values at 200 mJ become 0.9357, cannot reach the accuracy level at 50 and 100 mJ, but are better than at 150 mJ. At lower energies (50-100 mJ), the plasma is more stable and compressed or denser, or less dense, resulting in the minimized overlap of spectral lines and the consistent measurement of the spectrum. This is manifested through larger reverse R^2 values. At higher energies (150-200 mJ), the re-absorption and subsequent collision of electrons and other charged particles are possible and result in some deviation of the linear fit of the mathematical equation to the observations. This is presented in a moderately small R^2. From **Figure 4**, the low energy (50 mJ) case, the peak intensity is lower and the line amplitude is smaller. When the energy is 100 and 150 mJ, the peak intensity and amplitude are increased. At a higher fluence of 200 mJ, a broad strong peak is observed, reflecting more ions of atoms in the plasma. From **Figure 4,** the predominant wavelength might correspond to a particular constituent of the neem plant, like calcium (Ca), magnesium (Mg), or potassium (K). Higher energy results in being ionized, and the emission is brighter. Full Width at Half Maximum (FWHM) of the spectrum. The red horizontal lines denote the width at half maximum intensity (FWHM). The FWHM becomes larger with the increase of the laser power, which implies a higher plasma temperature and a larger influence of the spectral broadening.

Table 3. shows that each column is described as Laser energy (mJ). The applied values (50, 100, 150, 200 mJ) were representative of the considered laser energies impinging onto the sample. Electron temperature (eV): Electron temperature rises upon increasing the laser energy, meaning that the plasma is hotter at higher power. This rise implies the increased kinetic energy of the electrons, enhancing the collision in the plasma. Spectral line width (FWHM) $\Delta\lambda$ (nm). It corresponds to the amount that the spectral line would be seen with at half-maximum intensity, and is related to electron density, Doppler broadening, and collision. The spectral line amplitude follows laser energy upward, corresponding to higher plasma density and electron temperature in the process[22].

Electron Density (Number of Electrons per m^3): Tells you the number of free electrons in the plasma, and is an important parameter for the characterisation of the plasma. In other words, an increase in the power of the laser leads to higher ionization of the neem herb elements, and consequently, a higher number of free electrons. - Plasma Frequency: Represents the frequency of electron collective oscillation caused by electromagnetic forces in a plasma. It grows with the electron density, so the denser and more electrically transparent the plasma is, the higher the laser power is.

Debye Length (cm): The range in the plasma over which the electrostatic effects take place. There is a tradeoff between Fermi temperature and Fermi density, since the Debye length depends on both.

Debye Number: Denotes the number of electrons in the Debye sphere, governing the ionization and stability of the plasma. It tends to increase with the laser power, showing the plasma is more stable and ionized when high power is applied. Higher laser power results in higher electron temperature and plasma density. The spectral linewidth broadens with power as Doppler and

collisional broadening are enhanced. The plasma frequency scales linearly with the laser power and thus ionization of the sample. The Debye length is nearly constant, hence the plasma is stable and the equilibrium between density and temperature does not dramatically change. At higher energy (200 mJ), the plasma has a higher electron density, and the interaction between the laser and the sample was stronger.

Increasing laser power leads to increased plasma temperature and density. The FWHM line width of the spectrum is broadened, which means the collision and the Doppler effect have been enhanced. The higher plasma frequency corresponds to a more ionized plasma. The Debye length is about constant, leading to a temperature and density balance that is nearly stationary. As energy increases, the number of ND Debye particles also increases, which suggests a more stable plasma. In **Figure 5**, the left vertical axis (red) is associated with the line-n_e in units of 17 cm^{-3}.

The blue curve, represented on the right vertical axis in blue, is the electron temperature (Te) in eV. The red curve shows the evolution of the electron density (ne) with laser power. The blue curve exhibits the dependence of temperature (Te) on laser power. The electron number density and temperature increase as the laser intensity increases from 50 to 200 mJ, consistent with the theory of plasma formation in laser beam spectroscopy (LIBS). The increase in laser energy causes increase the absorption of energy by the target material (in this case, the neem material) and subsequent increase in the ionization, leading to the release of higher number of electrons, and then with higher numbers of electrons and more collision occurs between these charged particles that drives to the increase of the ne, and with higher numbers of electrons, we also have with a higher number of electrons, we have also more collisions between the charged particles, which lead to an increase in the electronic temperature (Te).

The non-linear growth of the curves has a higher slope at lower energy and decreases at higher energies, corresponding to ionization saturation at high laser energy. In the case of (Te), the incremental rate is lower than the electron density (ne) but has a consistent upward slope. Convergence of the values at 200 mJ for both 200 mJ laser energy, the values for (ne) and (Te) seem to be getting close to their upper limit of the thermal ionization region, indicating that the majority of the material has converted to a saturated plasma state. This implies that temperature or number density may not be significantly increased when the laser energy is higher than this, due to the equilibrium of ionization and recombination.

5. Conclusion

The study divulges that laser-induced breakdown spectroscopy (LIBS) is an efficient and direct technique to investigate the presence of elemental composition in neem (*Azadirachta indica*). Investigation in laser-generated plasma at various energies (50, 100, 150, and 200 mJ) upgraded our knowledge about the parameters that influence the plasma temperature and the electron density, thereby improving the accuracy of the spectroscopic analysis. The influence of the laser irradiation on plasma temperature and electron density was presented. As laser energy was increased, higher plasma temperatures and electron densities were obtained, which also reflect more excitation of the atomic species of the material sample. The Boltzmann equation that described the dependence of the plasma temperature on the laser energy and the Saha-Boltzmann equation that considered the influence of energy on the electron ionization were experimentally verified. The elemental composition of neem was determined, and it was found that the chemical composition of neem plasma includes several critical elements (Ca, Mg, K, Na), which are related to the physico-chemical properties during various applications and were expected to affect the efficacy of environmental and clinical uses. This demonstrates the utility of LIBS as a fast tool for determining the elements in an herbal drug. It is of great importance for the accurate analysis of data through adjusting the spectral parameters to choose the suitable laser power. Too low a power may not effectively activate the plasma, and too high a power may have undesirable effects such as excessive vaporization of the sample. Consequently,

optimization of the laser power levels and careful treatment of the spectral data are allowed, and the quality of measurements and the applicability of the LIBS technique in the investigation of organic substances are increased.

Acknowledgment

I would like to extend my thanks and appreciation to the Laboratory of Medical Physics at the College of Science for Women and to the professors working there for their assistance.

Conflict of Interest

The authors declare that they have no conflicts of interest.

Funding

There is no financial support for the submitted work.

Ethical Clearance

The procedures followed are consistent with ethical standards. The guidelines of the educational institution for research were followed.

References

1. Norazlina H, Suhaila A, Lili Shakirah H, Nurul Aniyyah MS. Green and free hazardous substances of neem oil lotions in promising market sustainability. Mater Today Proc. 2023. https://doi.org/10.1016/j.matpr.2023.01.017
2. Navale SS, Patil A. Herbal drugs used in various skin condition. Int J Novel Res Dev. 2023;8(2).
3. Parham S, Kharazi AZ, Bakhsheshi-Rad HR, Nur H, Ismail AF, Sharif S. Antioxidant, antimicrobial and antiviral properties of herbal materials. Antioxidants (Basel). 2020;9(12):1309. https://doi.org/10.3390/antiox9121309
4. Boanyah GY, Brenyah RC. The combined efficacy of neem (*Azadirachta indica*) seed oil and orange (*Citrus sinensis*) peel oil cream as a mosquito repellent. GSC Adv Res Rev. 2022;12(1):57–67. https://doi.org/10.30574/gscarr.2022.12.1.0184
5. Norazlina H, Muzammil MRAZ, Lili Shakirah H. Extraction of neem balm from *Azadirachta indica* leaves using Soxhlet method. Int J Synergy Eng Technol. 2024;5(1):36–46.
6. Marwa KJ, Aadim AK. Characteristics of lead and sulfur plasma parameters by optical emission spectroscopy. Iraqi J Sci. 2023;64(1):188–196. https://doi.org/10.24996/ijs.2023.64.1.19
7. Zaman MH, Rehman F, Tahir MS, Khan A, Amin N. Effect of preprocessing and normalization on classification of plant samples in machine learning assisted LIBS. Arab J Sci Eng. 2024;49(7):10003–10019. https://doi.org/10.1007/s13369-024-08716-0
8. Mahapatra PS, Dash S, Ratha S, Nayak PK, Mishra S, Sahu RK. Evaluation of medicinal plants using LIBS combined with chemometric techniques. Spectrochim Acta B. 2023;203:106738. https://doi.org/10.1016/j.sab.2023.106738
9. Huang T, Bi W, Song Y, Yu X, Wang L, Sun J, Jiang C. DMC-LIBSAS: A LIBS analysis system with double-multi convolutional neural network for accurate traceability of Chinese medicinal materials. Sensors. 2025;25:2104. https://doi.org/10.3390/s25072104
10. Cui X, Wang Q, Wei K, Teng G, Xu X. Laser-induced breakdown spectroscopy for classification of wood materials using machine learning with feature selection. Plasma Sci Technol. 2021;23(5). https://doi.org/10.1088/2058-6272/abf1ac
11. Kazim WA, Ali AH. Analysis of aloe vera plasma parameters using optical emission spectroscopy. Iraqi J Phys. 2025;23(1):44–54. https://doi.org/10.30723/ijp.v23i1.1306
12. Betlej I, Skrzeczanowski W, Nasiłowska B, Bombalska A, Borysiuk P, Nowacka M, Boruszewski P. Application of LIBS to determine graphene oxide incorporation on wood surfaces. Coatings. 2025;15(1):34. https://doi.org/10.3390/coatings15010034
13. Ahmed MA, Algwari QT, Younus MH. Plasma properties of a low-pressure hollow cathode DC discharge. Iraqi J Sci. 2022;63(6):2532–2539. https://doi.org/10.24996/ijs.2022.63.6.20

14. Wang YF, Zhu XM. Development of optical emission spectroscopy method with neural network model: determining electron density in xenon microwave discharge. J Appl Phys. 2024;136(24):243302. https://doi.org/10.1063/5.0243484
15. Mishra H, Tichý M, Kudrna P. OES study of plasma parameters in low-pressure hollow cathode plasma jet and planar magnetron. Vacuum. 2022;205:111413. https://doi.org/10.1016/j.vacuum.2022.111413
16. Ahmed AF, Mutlak FA, Abbas QA. Cold plasma effect for achieving fullerene and ZnO-fullerene hydrophobic thin films. Appl Phys A. 2022;128:147. https://doi.org/10.1007/s00339-021-05252-8
17. Iftikhar Y, Jamil N, Nazeer N, Tahir MS, Amin N. Optical emission spectroscopy of nickel-substituted cobalt–zinc ferrite. J Supercond Nov Magn. 2021;34(7):1–6. https://doi.org/10.1007/s10948-020-05734-5
18. Majeed NF, Ali AH, Mazhir SN, Akram RS. Effect of alum activated by cold plasma on mice wounds using textural analysis. Baghdad Sci J. 2024;21(12):4118–4127. https://doi.org/10.21123/bsj.2024.9026
19. Mullick A, Balagopalan S, Sooraj S, Karthikeyan B. Spectroscopic analysis of acid rain-induced stress in neem (*Azadirachta indica*). SSRN. 2025. https://doi.org/10.2139/ssrn.5187401
20. Alexandros S, Theofanis G, Emmanouil K, Kosmidis C. Identification of wood specimens utilizing fs-LIBS and machine learning techniques. Eur Phys J Appl Phys. 2024;99:11. https://doi.org/10.1051/epjap/2024230215
21. Ali AH, Shakir ZH, Mazher AN. Influence of cold plasma on sesame paste and nano sesame paste based on co-occurrence matrix. Baghdad Sci J. 2022;19(4):855. https://doi.org/10.21123/bsj.2022.19.4.0855
22. Elli B, Dimitris S, Nikos G. LIBS assisted by machine learning for olive oil classification. Spectrochim Acta B. 2019;163:105746. https://doi.org/10.1016/j.sab.2019.105746
23. Zaplotnik R, Primc G, Vesel A. Optical emission spectroscopy as a diagnostic tool for atmospheric plasma jets. Appl Sci. 2021;11(5):2275. https://doi.org/10.3390/app11052275
24. Karthigaikumar P, Justin VL. LIBS with neural network approach for plastic identification in waste management. Appl Chem Eng. 2024;7(1). https://doi.org/10.24294/ace.v7i1.3092
25. Rachdi L, Sushkov V, Hofmann M. OES diagnostics for plasma parameters in Duo-Plasmaline discharge. Spectrochim Acta B. 2022;194:106432. https://doi.org/10.1016/j.sab.2022.106432
26. Giannakaris N, Gürtler G, Stehrer T, Mair M, Pedarnig JD. OES of industrial atmospheric plasma jet: electron temperature study. Spectrochim Acta B. 2023;207:106736. https://doi.org/10.1016/j.sab.2023.106736
27. Mohsen M, Fatemeh R, Parvin KD. Hybrid machine learning algorithms for quantitative LIBS analysis. J Appl Spectrosc. 2023;90(3). https://doi.org/10.1007/s10812-023-01585-9
28. Datta R, Ahmed F, Hare JD. Machine-learning-assisted analysis of visible spectroscopy in pulsed-power plasmas. IEEE Trans Plasma Sci. 2024;52(10):4755–4763. https://doi.org/10.1109/TPS.2024.3364975
29. Sarsa A, Jiménez-Solano A, Dimitrijević MS, Yubero C. Exact Stark analytical function for Hα line related with plasma parameters. SSRN. 2025. https://doi.org/10.2139/ssrn.4786396
30. Oliver TA, Michoski C, Langendorf S, LaJoie A. Automated Bayesian estimation of plasma temperature and density from emission spectroscopy. Rev Sci Instrum. 2024;95(7):073520. https://doi.org/10.1063/5.0192810.